

Genetic noise mechanism for power-law switching in bacterial flagellar motors

M.I. Krivonosov¹, V. Zaburdaev^{1,3}, S.V. Denisov², and M.V. Ivanchenko^{2*}

¹*Institute of Supercomputing Technologies, Lobachevsky University, Nizhny Novgorod, Russia*

²*Department of Applied Mathematics, Lobachevsky University, Nizhny Novgorod, Russia*

³*Max Planck Institute for the Physics of Complex Systems, Dresden, Germany*

⁴*Institut für Physik, Universität Augsburg, D-86135 Augsburg, Germany*

Switching of the direction of flagella rotations is the key control mechanism governing the chemotactic activity of *E. coli* and many other bacteria. Power-law distributions of switching times are most peculiar because their emergence cannot be deduced from simple thermodynamic arguments. Recently it was suggested that by adding finite-time correlations into Gaussian fluctuations regulating the energy height of barrier between the two rotation states, it is possible to generate a switching statistics with an intermediate power law asymptotics. By using a simple model of a regulatory pathway, we demonstrate that the required amount of correlated ‘noise’ can be produced by finite number fluctuations of reacting protein molecules, a condition common to the intracellular chemistry. The corresponding power-law exponent appears as a tunable characteristic controlled by parameters of the regulatory pathway network such as equilibrium number of molecules, sensitivities, and the characteristic relaxation time.

PACS numbers: 87.10.P-e, 89.75.Da

I. INTRODUCTION

Bacteria are ubiquitous in nature, displaying a fascinating diversity in size, shape and habitat. Often, they cooperate to build colonies, also known as biofilms to adapt to changing and hostile environments [1]. Cells employ different strategies of taxis, sensitivity to temperature, chemical or electrical field gradients to vary direction of motion, reach favorable niches, and avoid harmful substances [2]. Among them, chemotaxis is probably best studied and its mechanisms are now understood quite well [3].

Locomotion of *E. coli* is the one of the most popular case study for bacterial swimming [4]. *E. coli* cells have several flagella that can rotate clockwise (CW) or counterclockwise (CCW). When all flagella are in a CCW rotation, they form a bundle and the cell performs a directed motion, often referred to as “run”. When one or several flagella switch to CW regime, the cell stops and begins to “tumble” [4]. During this stage *E. coli* chooses the direction of motion for the next run. The resulting angles are randomly distributed with the mean about 70° with respect to the direction of the previous run. A similar motility pattern is also found in a number of marine bacteria, for example *S. putrefaciens*, *P. haloplanktis* or *V. alginolyticus*, although they have a single flagella and the mean turning angle is often close to 180° , corresponding to reversals of the direction of motion [5].

Chemotactic strategies rely on controlling frequency of switching between CW and CCW rotations of bacterial motors: a favorable signal increases the intervals of directed motion. By regulating the duration of linear motion, bacteria perform a random walk biased towards (or away) the source of a chemical attractant (or repellent) [6]. In the absence of chemical gradients, durations of runs were commonly believed to be exponentially distributed [7]. However, recent advances in single cell tracking demonstrated strong cell to cell variability [8, 9], and, in observations of single motor rotations, even the power-law distributions were reported [6, 19].

The signaling pathway that modulates switching of individual flagellar motor rotation in response to a chemical signaling is well understood by now, and the corresponding biophysical models reproduce experimental observations quite successfully [6, 10]. However, the relative complexity of the full model, as well as some uncertainty about the influence of various intra- and extracellular processes, leave the question of the origin of the power-law distribution still open, to some extent. Moreover, to the best of our knowledge, power-law distributed runs were not yet observed experimentally with freely swimming bacteria [11].

Considerable progress in understanding the statistics of motor switching was achieved by means of a minimal model considering transitions between the two states over an energy barrier [14]. The regulating pathway was reduced to the action of the phosphorylated form of a signaling molecule, CheY-P, such that higher concentration of CheY-P leads to a higher probability of CCW to CW transition [15]. It was found, that Gaussian fluctuations with a finite correlation

*Electronic address: ivanchenko.mv@gmail.com

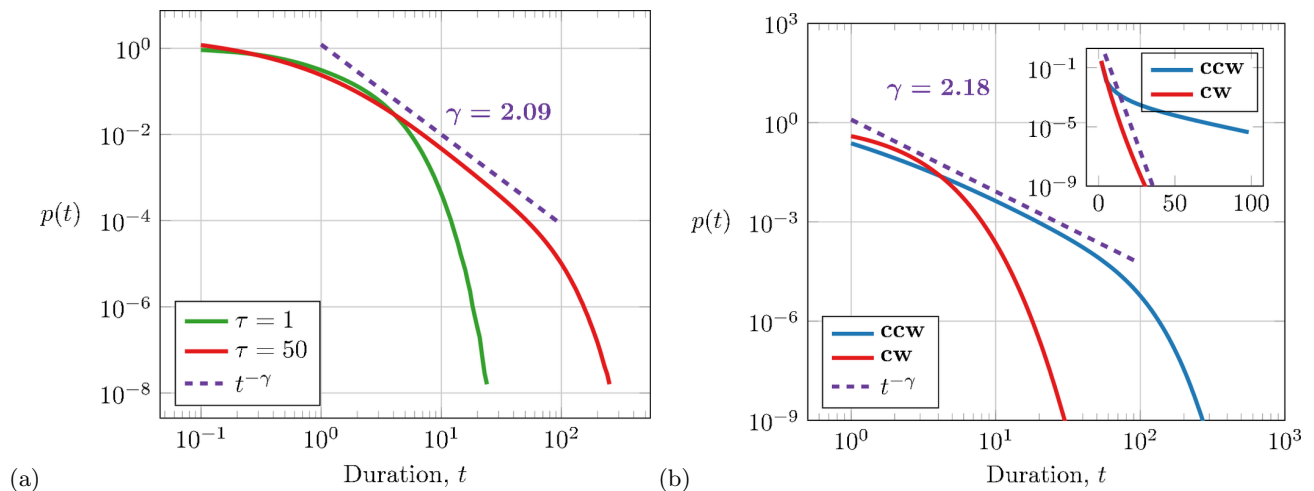


FIG. 1: (Color online) (a) Probability density functions of durations in the CCW state for different values of relaxation timescale of the CheY-P subsystem, τ . The other parameters are $\alpha = 10$, $Y_0 = 20$, and $K_0 = 1$; (b) Probability density functions of CW and CCW durations for $\alpha^+ = 1$, $\alpha^- = 10$, $Y_0 = 20$, $\tau = 50$, $K_0 = 1$. Dashed lines are power-laws with exponents $\gamma = 2.09$ (a) and 2.18 (b), which coefficient of determination is $R^2 = 0.98$, the number of samples is $N_{ccw} = N_{cw} = 10^{10}$, $t \in [1; 100]$. Inset: the same functions on a semi-log plot.

time in the height of these barriers can produce an algebraic scaling in the distribution of CCW durations [15]. These studies are in line with a broader research trend aimed at understanding of the genesis of power-law distributions in Langevin systems with multiplicative noise [16–18]. However, the origin of such fluctuations was not well-established in Ref. [15]. It was conjectured that intrinsic stochasticity of the regulating genetic pathway, in particular, ‘genetic noise’ due to a finite number of reacting protein molecules in the cell could produce such fluctuations.

In this paper, we investigate this hypothesis by using chemical kinetics models of CheY-P synthesis and resulting CCW – CW switching. We demonstrate that molecular noise and its correlations due to finite regulator protein synthesis timescales are sufficient to reproduce distribution of CCW durations with intermediate power-law asymptotics. Complementary exponential distributions of CW durations are consequence of a weaker sensitivity of CW – CCW transition threshold to CheY-P regulation.

The paper is organized as follows: In Section II, we formulate two models of CheY-P regulating pathways, specify the corresponding rates, and briefly discuss meaning of model parameters. In Section III, we present the results of a massive numerical sampling obtained by implementing Gillespie stochastic algorithm. An alternative approach, based on the so-called full-counting statistics, which allows us to avoid resource expensive sampling and extract the probability distribution functions for CCW and CW durations directly from the chemical rates, is presented in Section IV. We conclude the paper with some discussion in Section V.

II. MODELS

Chemotactic regulation of *E. coli* relies on the complex intracellular signaling network [19]. It starts with chemoreceptors at cytoplasmic membrane, the binding sites for chemoattractant molecules. The intracellular transduction cascade controls production of CheY-P protein that diffuses to motors and modulates switching of the direction of rotation, CW or CCW, making bacteria tumble or run.

A minimal model of the regulatory pathway is given in terms of chemical kinetics. Transitions between states with different number of CheY-P molecules, Y , follow



where $K_y^+ = \frac{Y_0}{\tau}$, $K_y^- = \frac{Y+1}{\tau}$ are transition rates, Y_0 is the equilibrium number of molecules, and τ is the characteristic relaxation time of the signaling pathway. Being an elementary birth-death process, it intrinsically contains all necessary ingredients, stochasticity, discreteness of states and finite correlation time, τ , which previously had to be brought in by an additive Gaussian noise [14]. We assume that concentration of chemoattractant, the input signal for the pathway,

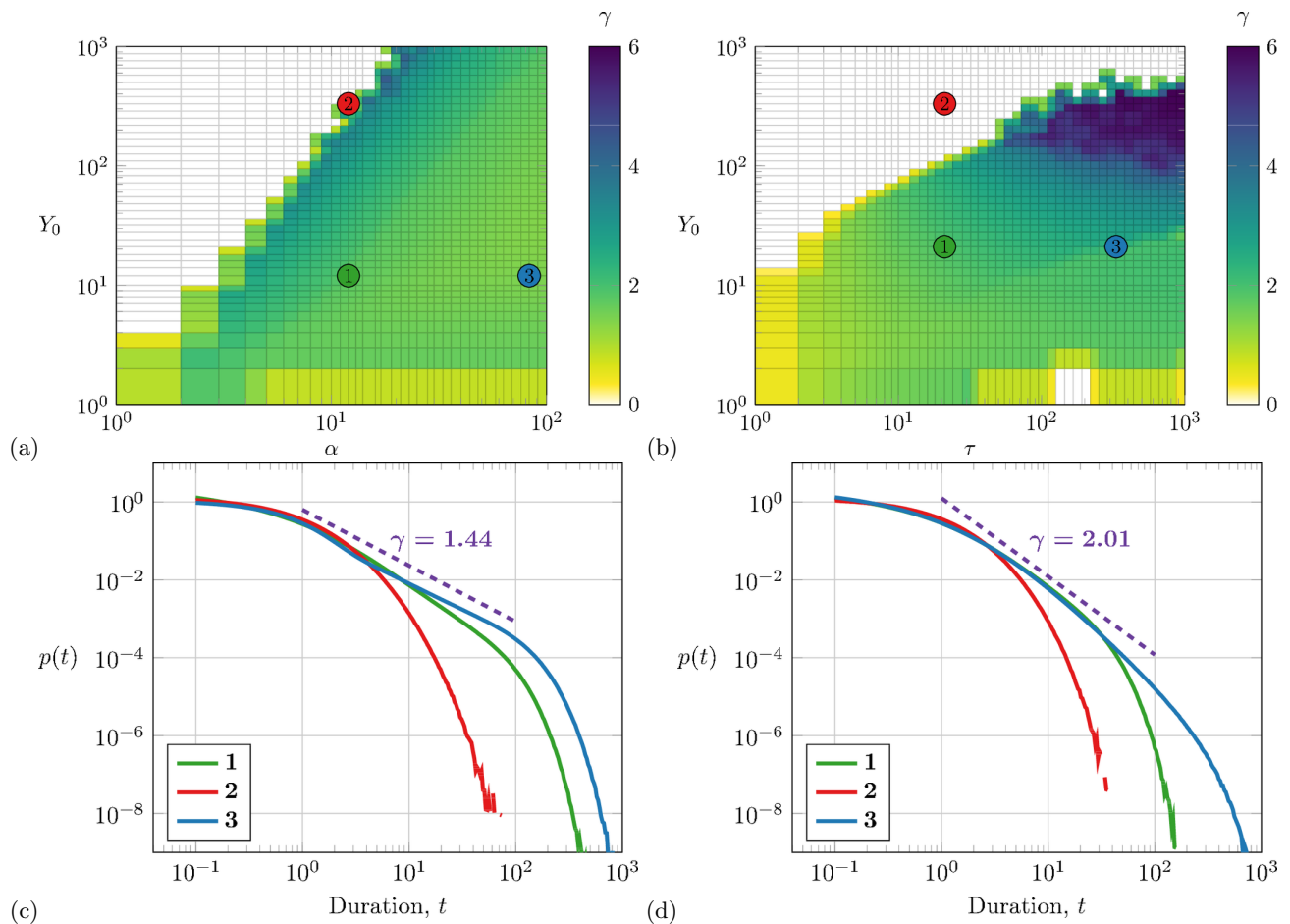


FIG. 2: (Color online) Power law exponent γ for the probability density functions (PDFs) of CCW durations (color coded) as function of the mean number of CheY-P molecules, Y_0 and sensitivity α [for fixed $\tau = 50$] (a) or correlation time τ [for fixed $\alpha = 10$ and $K_0 = 1$] (b). In the white area the power law fit for duration distributions does not pass the quality test (cf. Models and Methods for details.) PDFs for the points marked on panel (a, b) are shown on panels (c, d), respectively.

is changing slowly (in course of motion of a cell in the gradient or time variations of its level), as compared to the switching timescale, so that Y_0 can be taken constant.

Switching of flagella rotations is also modeled from the first principles. Let $X = 0$ correspond to the clockwise and $X = 1$ to the counterclockwise regimes. Transitions are controlled by the state of the regulating pathway, Y [14]



where $K_x^+ = K^+(1 - X)$, $K_x^- = K^-X$, formally restricting transitions to the set of two states $X = \{0, 1\}$. The transition rates are modulated by the level of CheY-P:

$$K^\pm = K_0 \exp\left(\pm \alpha^\pm \frac{Y_0 - Y}{Y_0}\right), \quad (3)$$

where $\alpha^\pm > 0$ set sensitivities, and the energy barriers are approximated by a linear dependence on CheY-P level [15].

Let us discuss the qualitative behavior of the model. Assume that a flagellum rotates clockwise (tumbling), such that $X = 0$, then $K_x^+ = K^+$, $K_x^- = 0$. If the level of CheY-P goes below the equilibrium value, $Y < Y_0$, then the rate coefficient $K^+ > K_0$ and switching to counterclockwise rotation (running) will be favoured. Conversely, higher levels of Che-P, $Y > Y_0$, will delay the switch. When a flagellum rotates counterclockwise (run), respective fluctuations above and below an equilibrium value Y_0 will lead to the opposite effects. Non-identical sensitivities to the regulating signal, α^\pm , allow for independent tuning of the transition rates between running and tumbling.

The above simple model has one drawback, that is transition rates in Eq.(3) can get exponentially large (small) in response to increasing (decreasing) signal Y , which may be not biologically plausible. To account for a finite capacity of CheY-P – motor protein binding, the rates can be modified as suggested in Ref. [10]:

$$K^\pm = K_0^\pm \exp \left[\pm \frac{\alpha^\pm}{2} \left(\frac{1}{2} - \frac{Y}{Y + K_d} \right) \right], \quad (4)$$

which corresponds to saturation with the level of Y_n above the dissociation constant K_d .

III. RESULTS OF THE STOCHASTIC SAMPLING

We first perform numerical simulations of the models (1-4) by implementing Gillespie stochastic algorithm [20], thereby making the study free of any kind of approximation in terms of deterministic mean-field equations or continuous-state (Langevin) approximations [10, 14]. Each realization corresponds to $N = 10^7$ steps of the algorithm (one of a possible set of chemical reactions). The durations of residence in each state, t_{ccw} and t_{cw} , are determined as the time between two consecutive relevant reactions. At least $N_{cw} = N_{ccw} = 10^{10}$ durations of CW and CCW states are collected in repeated realizations to calculate their probability distribution functions (PDFs), $p(t_{cw})$ and $p(t_{ccw})$, and analyze their dependence on the relaxation (correlation) time of the regulatory signal and the sensitivity of transition rates.

The power-law fitting of the obtained PDFs is then performed by using the least squares linear regression for the log-log scaled distributions. The quality of fit is characterized by the coefficient of determination [21], $R^2 \in [0, 1]$, with large values corresponding to better fit. We vary the interval of durations to search for the best fit, l , and request that it spans over at least 1.3 decades with $R^2 > 0.98$. Otherwise, the power law hypothesis is rejected.

We start with the simplest form of rate coefficients, as given by Eq. (3), and estimate PDFs of durations of run and tumble phases. It is straightforward to see that if CheY-P is absent, $Y_0 = 0$ (switching is insensitive to CheY-P, $\alpha^\pm = 0$), the process is Poissonian and the PDFs of residence intervals are exponential, $p(t_{ccw}), p(t_{cw}) \propto \exp(-K_0 t)$.

We begin with the case of equal sensitivities, $\alpha^\pm = \alpha$. Numerical results indicate that a correlated molecular noise due to the pathway signal, Y , can produce an algebraic scaling in distributions of durations, $p(t_{ccw}) \propto t^{-\gamma}$, over a pronounced interval (1.5 – 2 decades) with the cutoff at large durations; see Fig. 1(a). PDFs with intermediate power-law asymptotics extending over $\lesssim 2$ decades and then damped with a near exponential cut-off are typical to both *in vivo* and *in vitro* measurements of bacteria and cell spatial activities; see, e.g., Refs. [19, 22].

In accordance with Ref. [14], decreasing the correlation time changes this distribution towards an exponential. The model is also capable of reproducing the exponential statistics for CW durations, coexisting with the power law scaling for CCW durations. The only source of non-identity is in the sensitivity of transition rates to signaling, $\alpha^+ \neq \alpha^-$. As the residence time in a state is determined by the escape rate, it can be expected that a decreased sensitivity of CW \rightarrow CCW transition to the level of CheY-P, will lead to an exponential distribution of CW durations (as in the limiting case $\alpha^+ = 0$). An example of this regime is shown in Fig. 1(b).

Extensive simulations in a large parameter region reveal that power law distributions emerge only when the relaxation timescale of CheY-P level is substantially greater than that of switching between CW and CCW states, $\tau \gg 1/K_0$, see Fig. 2. At the same time, we observe that the increase of the mean number of signaling molecules, Y_0 , destroys power law scaling, see Fig. 2(a). This effect can be understood as diminishing of the fluctuations with large numbers of reacting molecules. Sensitivity parameter, α , is also able to control transition between power law and exponential PDFs of duration intervals (Fig. 2(b)). Values of the power-law exponent found in most of the region, $1 < \gamma < 2$, are consistent with experimental observations, which estimated the power law exponent for the cumulative distribution of CCW durations as $\gamma - 1 \approx 1.5$, and evidence that slow methylation as a part of the signaling pathway, is responsible for the long time correlations in the signal output that could stand behind the power law [19].

Now we consider a more biologically plausible model for transition rates, Eq. (4), that captures saturation in the motor response. To sharpen the effect, we turn to the case $K_d < Y_0$, when saturation is pronounced already on the equilibrium level of CheY-P, $Y_p = Y_0$. Our results confirm that again slow relaxation and long correlations in Y_p , together with higher sensitivity of the CCW \rightarrow CW transition to the regulatory signal, can lead to the appearance of a power law asymptotics in the PDF of CCW durations, while CW durations remain exponentially distributed, see Fig.3.

A systematic study of statistics as a function of the parameter values of the model is presented in Fig. 4. The (K_d, Y_0) parameter plane exhibits two different regions, Fig. 4(a). Namely, for $Y_0 < K_d$, when saturation effects are weak, there is a strong deviation from the power-law statistics as the number of molecules increases. Power law scaling appears with relatively low numbers, $\gamma < 2$. For $Y_0 > K_d$ saturation effects make the exponent to reach larger values, $\gamma > 4$.

On other parameter plane, (K_d, α^-) , we observe a persistence of the power-law scaling in a large range of CCW \rightarrow CW transition sensitivities, α^- , Fig.4(b). There, one again notices the regimes with relatively small, $\gamma \leq 2$, and large,

$\gamma > 4$, values of the power law exponent, as dictated by the ratio between the mean number of CheY-P molecules, Y_0 , and the saturation constant K_d .

IV. SWITCHING TIME DISTRIBUTIONS FROM FULL-COUNTING STATISTICS

Costly numerical sampling can be avoided by implementing the toolbox of full-counting statistics [23]. Originally introduced in the context of quantum transport [24], this formalism applies to all master equations, independent of their genesis [25]. Here we demonstrate how it can be used to extract switching statistics directly from transition rates $K_x^\pm(Y)$ and $K_y^\pm(Y)$.

The kinetics of the models (1 - 2) can be evaluated in terms of continuous-time Markov process [26]; the corresponding transition diagram is shown in Fig. 5a. A state $Z(t)$ of the process at time t is a two-dimensional vector, $Z = \{X, Y\}$ with first binary component representing the rotational regime, $X = 0$ (CW) and $X = 1$ (CCW), and the second one, Y , being the number of CheY-P molecules. The corresponding master equation for the probability vector $P(Z, t) \equiv P(X, Y; t)$ has the form

$$\begin{aligned} \dot{P}(0, 0; t) &= -\left[\frac{Y_0}{\tau} + K_x^+(0)\right]P(0, 0; t) + K_x^-(0)P(1, 0; t) + \frac{1}{\tau}P(0, 1; t) \\ \dot{P}(1, 0; t) &= -\left[\frac{Y_0}{\tau} + K_x^-(0)\right]P(1, 0; t) + K_x^+(0)P(0, 0; t) + \frac{1}{\tau}P(1, 1; t) \\ &\dots \\ &\dots \\ &\dots \\ \dot{P}(0, Y; t) &= -\left[\frac{Y_0 + Y}{\tau} + K_x^+(Y)\right]P(0, Y; t) + K_x^-(Y)P(1, Y; t) + \frac{Y + 1}{\tau}P(0, Y + 1; t) + \frac{Y_0}{\tau}P(0, Y - 1; t) \\ \dot{P}(1, Y; t) &= -\left[\frac{Y_0 + Y}{\tau} + K_x^-(Y)\right]P(1, Y; t) + K_x^+(Y)P(0, Y; t) + \frac{Y + 1}{\tau}P(1, Y + 1; t) + \frac{Y_0}{\tau}P(1, Y - 1; t) \\ &\dots \end{aligned} \quad (5)$$

It is noteworthy that our model serves a generalization of a fluid queue driven by a birth-death process proposed by van Doorn, Jagers, and de Wit [27]. Namely, in the framework of Markov processes, reaction (2) is an exchange of probability between two states; it can be considered as an exchange of a fixed amount of an incompressible fluid between two tanks at rates determined by the state of a birth-death process (in the original formulation there was only one infinite-volume tank and unlimited amount of fluid). A CCW duration is a time a single (marked) molecule of fluid spends in the tank “1” before leaving it. By introducing a probability vector $\mathbf{P}(t) = \{P(X = 0, Y = 0; t), P(X = 0, Y = 1; t), P(X = 0, Y = 2; t), \dots, P(X = 1, Y = 0; t), P(X = 1, Y = 1; t), P(X = 1, Y = 2; t), \dots\}$ and a transition

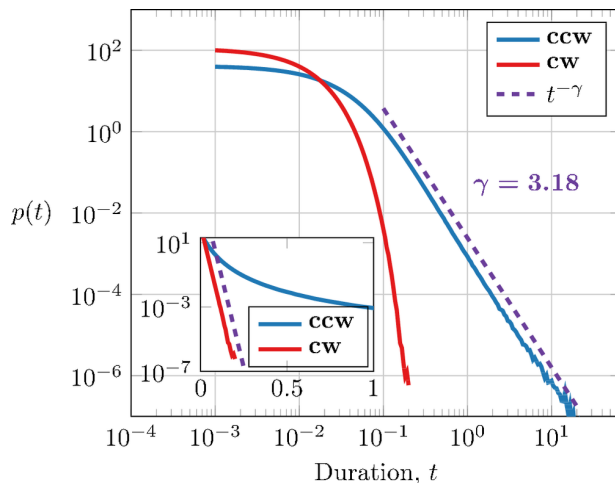


FIG. 3: (Color online) Probability density functions of CW and CCW durations for $\alpha^- = 30, \alpha^+ = 1, Y_0 = 10, \tau = 50, K_d = 2, K_0^+ = 100, K_0^- = 0.2$. Dashed line is a power-law with $\gamma = 3.18, R^2 = 0.999, N_{ccw} = 10^{11}, t \in [0.1; 20]$. Inset: the same distributions in the semi-log plot.

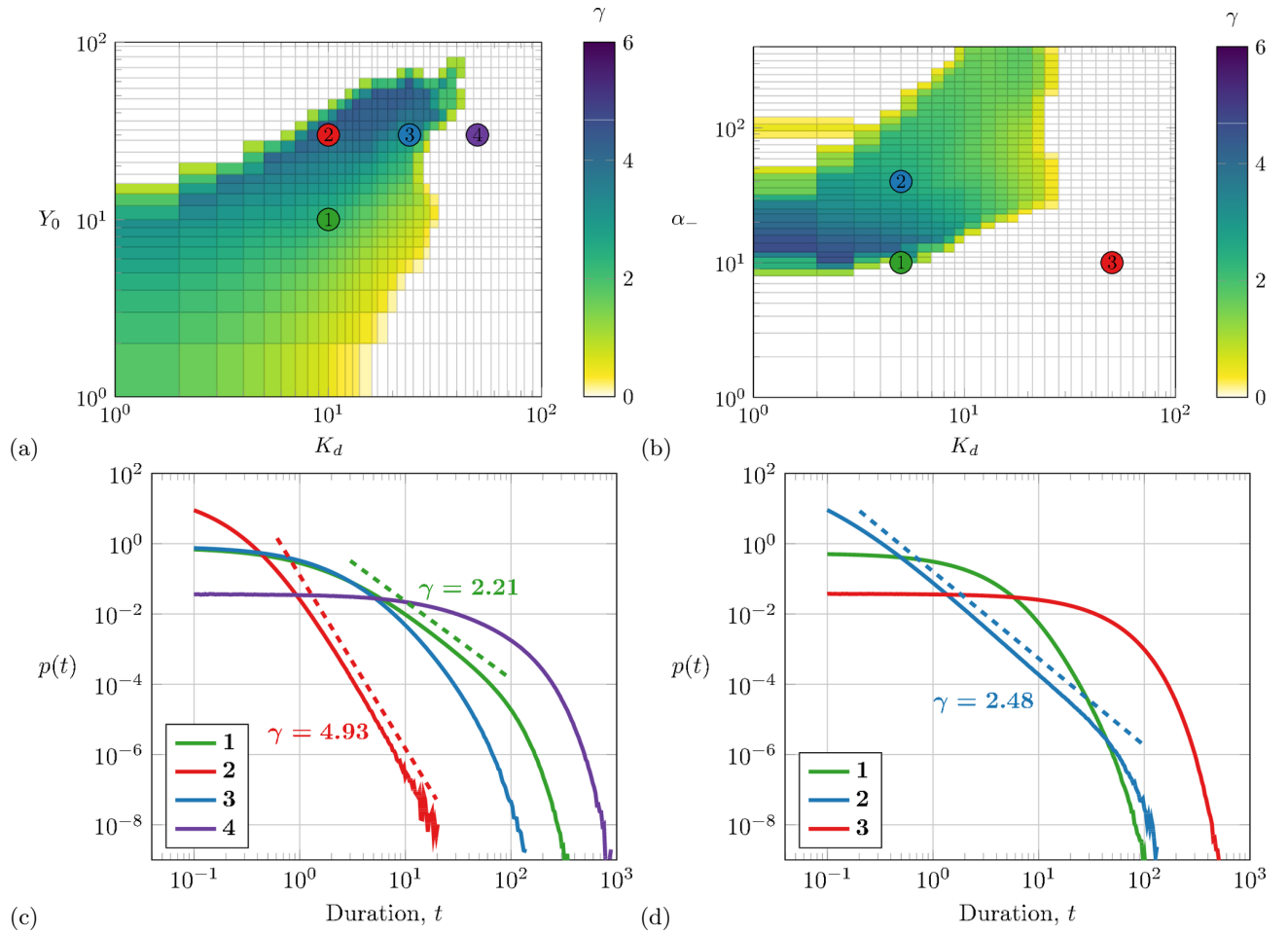


FIG. 4: (Color online) Power law exponent γ estimated for the PDFs of CCW durations (color coded) as function of saturation constant, K_d , and (a) mean number of CheY-P molecules, Y_0 , for fixed $\alpha^- = 30$ and (b) sensitivity α^- for fixed $Y_0 = 10$. The other parameters are $\alpha_+ = 1$, $\tau = 50$, $K_{+0} = 100$, $K_{-0} = 0.2$. In white area, the power law fit for the PDFs does not pass the quality test (cf. Models and Methods for details.) PDFs for the points marked on panel (a, b) are shown on panels (c, d), respectively.

rate matrix \mathbf{Q} [26], we can re-write equation (6) in a compact form, $\dot{\mathbf{P}}(t) = \mathbf{Q}\mathbf{P}(t)$. Matrix \mathbf{Q} consists of two identical semi-infinite diagonal blocks $\tilde{\mathbf{Q}}_{\text{BD}}$ [matrices of the tridiagonal form and consisting of the rates of the birth-death process] accompanied with off-diagonal blocks $-\tilde{\mathbf{Q}}_{01(10)}$ [matrices of the diagonal form, with entries $K_x^+(Y)$ ($K_x^-(Y)$)].

Next we consider the probability $\mathcal{P}(t)$ of no transition occurred from state 1 to state 0 during time t . This probability is specific to the initial distribution $\mathbf{P}_{\text{entry}} \equiv \{P_{\text{entry}}(Y)\}$, $P_{\text{entry}}(Y) := P(1, Y, 0)$ (the meaning of this notation will be apparent soon). For a chosen initial state, $\mathcal{P}(t)$ can be calculated from the state vector $\mathbf{P}^{(0)}(t) \equiv \{P^{(0)}(Y; t)\}$ (here superscript (0) denotes number of transitions on which the state is conditioned [25]). The evolution of this vector is governed by the master equation

$$\dot{\mathbf{P}}^{(0)}(t) = \tilde{\mathbf{Q}}_{\text{NT}}\mathbf{P}^{(0)}(t) = [\tilde{\mathbf{Q}}_{\text{BD}} - \tilde{\mathbf{Q}}_{10}]\mathbf{P}^{(0)}(t). \quad (6)$$

The no-transition probability is then $\mathcal{P}(t) = \sum_Y P^{(0)}(Y; t)$.

Matrix $\tilde{\mathbf{Q}}_{\text{NT}}$ is a semi-infinite Jacobi matrix, i.e., it is a tridiagonal matrix with positive off-diagonal entries. Therefore, it has a purely real non-degenerated spectrum, $\{\lambda_1, \lambda_2, \dots, \lambda_i, \dots\}$. The largest eigenvalue is negative, $\lambda_1 < 0$ [there is a 'leak' from state $X = 1$ to state $X = 0$ so that master equation (6) does not preserve the vector norm] and, therefore, $\forall \lambda_i < 0$. The conditioned probability vector at any instant of time can be obtained by implementing spectral decomposition, $\mathbf{P}^{(0)}(t) = \sum_i \alpha_i \exp(\lambda_i t) \cdot \mathbf{v}_i$, where $\alpha_i = \mathbf{w}_i^T \cdot \mathbf{P}_{\text{entry}}$ and $\{\mathbf{w}_i, \mathbf{v}_i\}$ is the dual left-right eigenset of $\tilde{\mathbf{Q}}_{\text{NT}}$. The decay of $\mathcal{P}(t)$ is monotonous due to the properties of the spectrum.

Finally, to calculate $p(t)$ for the CCW phase, we need to calculate $\mathcal{P}(t)$ for the initial vector $\mathbf{P}_{\text{entry}}$ corresponding to the distribution over Y states at the moment when the transition $X = 0 \rightarrow X = 1$ happens. In this case

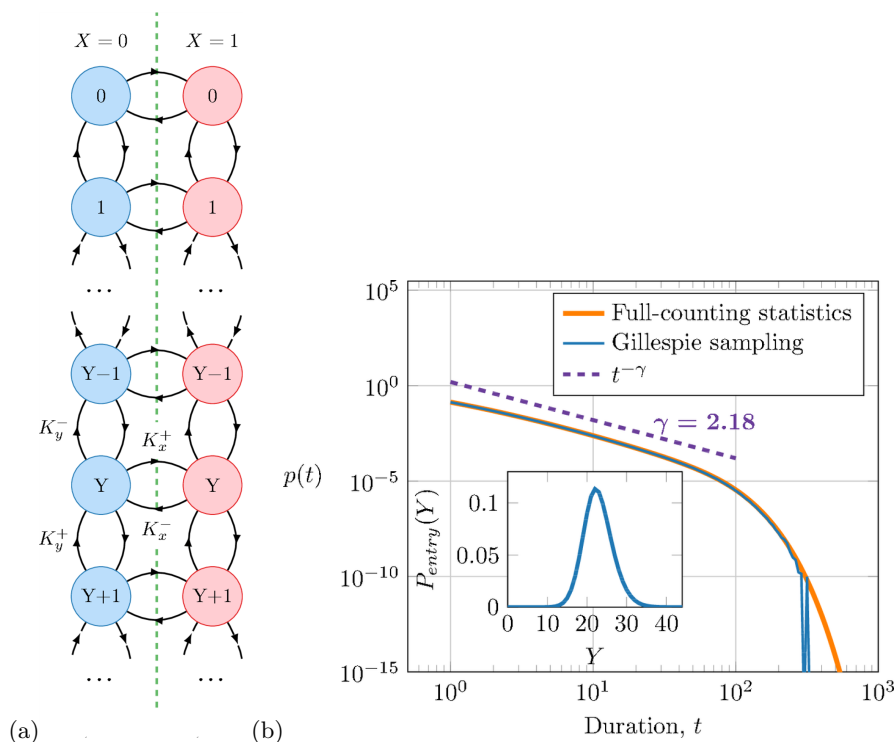


FIG. 5: (Color online) (a) Transition diagram for the process (1-2). (b) Probability density functions of CCW durations obtained from full-counting statistics of the process described by the master equation Eq. (6) with truncation at $Y_{max} = 100$ (thick orange line) compared to the results of Gillespie sampling (blue line). The inset shows the probability distribution $P_{\text{entry}}(Y)$ for the entry distribution of the CCW phase, Eq. (7). Other parameters are the same as in Fig. 1b.

$$p(t) = -\dot{P}(t) = \sum_i \alpha_i \cdot (-\lambda_i) \cdot \exp(\lambda_i t) \cdot \mathbf{v}_i.$$

The entry distribution, in its turn, can be obtained from the stationary distribution \mathbf{P}_{st} of the full Markov evolution, $\mathbb{Q}\mathbf{P}_{st} = \mathbf{0}$, by taking only $X = 0$ sub-vector, $\{P_{st}(X = 0, Y)\}$, which defines the probability to find the system in a state Y conditioned on that the system is in the set $X = 0$. Next we should multiply this probability with the probability that the reaction which takes the system into the set $X = 1$ will happen when the system is in the state $\{X = 0, Y\}$. This probability is proportional to $K_x^+(Y)$ [28], so we have

$$P_{\text{entry}}(Y) = P_{st}(X = 0, Y) \cdot K_x^+(Y) / \text{Norm}[P_{st}(X = 0, Y) \cdot K_x^+(Y)], \quad (7)$$

Practically, it means that all needed ingredients – (i) the spectrum and eigenset of $\tilde{\mathbb{Q}}_{NT}$ and (ii) the stationary distribution of \mathbb{Q} – can be obtained by truncating the state space with some Y_{max} and performing two routine matrix diagonalizations, of the size Y_{max} and $2Y_{max}$, respectively. A realization of this recipe is presented in Fig. 5b. Thus calculated distribution $p(t)$ perfectly matches the distribution obtained by performing Gillespie sampling.

V. CONCLUSIONS

We studied statistics of flagella switching between CCW (‘run’) and CW (‘tumble’) regimes, the output of chemotactic signaling pathway controlled by the molecular dynamics of CheY-P protein. We demonstrated that the correlated noise induced by finite-size fluctuations is sufficient to reproduce distributions of CCW durations with intermediate power-law asymptotics in a broad parameter region. Extensive numerical sampling allowed us to map parameter regions with power law statistics and define the values of the corresponding exponents.

While the precise mechanism behind the observed power-law asymptotics needs to be further investigated, their origin can be intuitively understood from the Markov interpretation; see Fig. 5a. Namely, it is the presence of hidden variable Y which supervises the transition rates between the two X states (otherwise, in the absence of Y , $p(t)$ would be a plain exponential distribution). We conjecture that this mechanism is somehow related to the recent deduction of Zip’s law for statistical models with hidden (‘unobservable’, ‘latent’, etc) variables [30]. Hidden variables ‘mix’ together many different reactions (processes, pathways, etc) that individually do not obey Zip’s law in a such way that

the resulting mixture obeys this law. This mechanism is an interesting alternative to the prevailing (at the moment) approach based on the fine parameter tuning into criticality. Zipf's law, roughly speaking, corresponds to the case with exponent $\gamma = 1$. How this new approach can be generalized – within the chemical kinetics framework – to the case with tunable exponents is a challenging question.

Our results open certain theoretical perspectives. The origin of power-law distributions found in mobility patterns of many living organisms, ranging from bacteria to sharks and human beings, remains a mystery [31]. Even though one can accept the hypothesis that this type of distributions was selected by evolution as the optimal strategy for survival and best accomplishment of every-day routines, physiological mechanisms behind the power-laws are not understood yet. A simple chemical network, driven by finite number fluctuations intrinsic to intracellular molecular dynamics, is able to generate tunable power-law distributions and therefore constitutes a promising candidate for such a 'generator'. Our findings are also of potential relevance to bioengineered cell chemotaxis (to control motility of bacteria), biofilms formation and targeted cell-assisted drug delivery.

VI. ACKNOWLEDGMENTS

This work was supported by the Russian Science Foundation grant No. 16-12-10496 (M.K., S.D. and V.Z.).

-
- [1] G. O'Toole, H.B. Kaplan, R. Kolter, *Biofilm formation as microbial development*, Annu. Rev. Microbiol. **54**, 49 (2000).
 - [2] M. Eisenbach, *Chemotaxis*, London: Imperial College Press **1**, 499 (2004).
 - [3] G. L. Hazelbauer, *Bacterial chemotaxis: The early years of molecular studies*, Annu. Rev. Microbiol. **66**, 285 (2012).
 - [4] L. Turner, W. S. Ryu, H. C. Berg, *Real-time imaging of fluorescent flagellar filaments*, J. Bacteriol. **182(10)**, 2793 (2000).
 - [5] G. M. Barbara, J. G. Mitchell, *Bacterial tracking of motile algae*, FEMS Microbiol. Ecol. **44**, 79 (2003).
 - [6] Y. Tu, *Quantitative modeling of bacterial chemotaxis: Signal amplification and accurate adaptation*, Annu. Rev. Biophys. **42(1)**, 337 (2013).
 - [7] S. M. Block, J. E. Segall, H. C. Berg, *Adaptation kinetics in bacterial chemotaxis*, J. Bacteriology **154(1)**, 312 (1983).
 - [8] Y. Dufour, S. Gillet, N. Frankel, D. Weibel, T. Emonet, *Direct correlation between motile behavior and protein abundance in single cells*, PLOS Comp. Biology **12**, e1005041 (2016).
 - [9] H. Berg and D. Brown, *Chemotaxis in Escherichia coli analysed by three-dimensional Tracking*, Nature **239**, 500 (1972).
 - [10] N. W. Frankel, W. Pontius, Y. S. Dufour, J. Long, L. Hernandez-Nunez, T. Emonet, *Adaptability of non-genetic diversity in bacterial chemotaxis*, eLife **3**, e03526 (2014).
 - [11] Most of the collected experimental data are in agreement with the exponential run time distribution. There are several models which exhibit this type of run time distributions; see e.g., Refs. [12, 13].
 - [12] R. Grossmann, F. Peruani, and M. Bär, *Diffusion properties of active particles with directional reversal*, New J. Phys. **18**, (2016).
 - [13] M. Theves, J. Taktikos, V. Zaburdaev, H. Stark, and C. Beta, *A bacterial swimmer with two alternating speeds of propagation*, Biophys J. **105**, 1915 (2013).
 - [14] Y. Tu and G. Grinstein, *How white noise generates power-law switching in bacterial flagellar motors*, Phys. Rev. Lett. **94**, 208101 (2005).
 - [15] S. Khan, R. M. Macnab, *The steady-state counterclockwise/clockwise ratio of bacterial flagellar motors is regulated by protonmotive force*, J. Mol. Biol. **138(3)**, 563597 (1980).
 - [16] D. Sornette, *Critical Phenomena in Natural Science*, (Springer, N.Y., 2006).
 - [17] T. S. Bir and A. Jakovac, *Power-law tails from multiplicative noise*, Phys Rev. Lett. **94**, 132302 (2005).
 - [18] S. Morita, *Power-law exponent in multiplicative Langevin equation with temporally correlated noise*, arXiv:1709.05620v2 (2017).
 - [19] E. Korobkova, T. Emonet, J. Vilar, T. Shimizu, and P. Cluzel, *From molecular noise to behavioural variability in a single bacterium*, Nature **428(6982)**, 574 (2004).
 - [20] D. Gillespie, *Stochastic simulation of chemical kinetics*, Annu. Rev. Phys. Chem. **58(1)**, 35 (2007).
 - [21] N.R. Draper, H. Smith, *Applied Regression Analysis*, (Wiley Series in Probability and Statistics, N.Y., 1998).
 - [22] T. H. Harris *et al.*, *Generalized Lévy walks and the role of chemokines in migration of effector CD8+ T cells*, Nature **486**, 545 (2012).
 - [23] M. Esposito, U. Harbola, and S. Mukamel, *Nonequilibrium fluctuations, fluctuation theorems, and counting statistics in quantum systems*, Rev. Mod. Phys. **81**, 1665 (2009).
 - [24] L. S. Levitov and G. B. Lesovik, *Charge-distribution in quantum shot-noise*, JETP Lett **58**, 230 (1993); L. S. Levitov, H. W. Lee, and G. B. Lesovik, *Electron counting statistics and coherent states of electric current*, J. Math. Phys. **37**, 4845 (1996).
 - [25] U. Mordovina and C. Emary, *Full-counting statistics of random transition-rate matrices*, Phys. Rev. E **88**, 062148 (2013).
 - [26] W. Anderson, *Continuous-time Markov chains: An Applications-Oriented Approach* (Springer, New York, 1991).
 - [27] E. A. van Doorn, A. A. Jagers and J. S. J. de Wit, *A fluid reservoir regulated by a birth-death process*, Stoch. Mod. **4**, 457 (1988).

- [28] Formally speaking, this probability is $K_x^+(Y)/\sum_S K_x^+(S)$ and it is impossible to define it for a system with an infinite number of states (which is our case). However, this problem can be circumvented by taking into account that the distribution of probability over the entry states [accounted with $P_{st}(X=0, Y)$] is localized in a small subset of Y states (for more precise definition see Ref. [29]). Then the consideration can be reduced to a system with a *finite* number of states where the normalization of reaction probabilities is indeed possible. Since we need only the final answer, Eq. (6), we simply adsorb all this in the normalization of the vector \mathbf{P}_{entry} .
- [29] B. Munsky and M. Khammash, *The finite state projection algorithm for the solution of the chemical master equation*, J. Chem. Phys. 124, 044104 (2006).
- [30] D. J. Schwab, I. Nemenman, and P. Mehta, *Zipf's law and criticality in multivariate data without fine-tuning*, Phys. Rev. Lett. **113**, 068102 (2014).
- [31] V. Zaburdaev, S. Denisov, J. Klafter, *Lévy walks*, Rev. Mod. Phys. **87**, 483-530 (2015).